A combined sparse-spatial representation image fusion method

Nannan Yu

School of Electrical Engineering and Automation, Jiangsu Normal University, Xuzhou 221116, China

yunannan1981@126.com

Abstract

The existing image fusion methods can be classified into the spatial domain and the transform domain techniques. Every type of techniques has its advantages and shortcomings. In this paper, we intend to carry forward their advantages and overcome their shortcomings by combining the fusion techniques of the spatial domain and the transform domain, and a combined sparse-spatial representation method is proposed. Our method seeks a sparse representation (SR) for each patch of all source images, and then uses the sparse coefficients and the composite dictionary to generate the fused image. Other than the existing SR-based fusion methods, our method considers the atoms of dictionaries as the image features, instead of the coefficients. The atoms of dictionary represent the essence elements of the images and the dimension of dictionary is usually less than that of coefficient matrix, so our method can combine the essence elements of the images while could offer a reduction in the computational complexity. Since SR has stronger ability to remove noise, our method is naturally robust to noise. Experiment results show that the performance of the proposed method is better than that of other methods in terms of several metrics, as well as in the visual quality.

Keywords

Image fusion, sparse representation, dictionary.

1. Introduction

Image fusion integrates redundant as well as complementary information present in source images in such a manner that the fused image describes the true source better than any of the individual image. The exploitation of redundant and complementary information improves the accuracy, reliability and interpretability of the images. Image fusion has been used widely in various areas of image processing, such as remote sensing for combining high-resolution panchromatic and low-resolution multispectral images, medical diagnosis for obtaining images having both soft issue and hard issue information, and target recognition for combining visible and infrared images [1], [2], [3].

From the 1980s to now, the image fusion technology has aroused extensively interests and resulted in plenty of achievements. Nikolov *et al.* propose a classification of image fusion algorithms into the spatial domain and the transform domain techniques [4]. The spatial domain techniques use the source image itself (or partial image) as image features, and combine the features with the fusion rule. Aslantas *et al.* [5] propose a spatial domain multi-focus image fusion algorithm and choose the sharper image blocks within the source images to construct the fused image. Maruthi *et al.* [6] use the measure of fuzziness to determine the activity indicator, and select the image blocks with the largest activity indicator. Stathaki and Mitianoudis in [7] propose two spatial domain methods: the Dispersion Minimisation Fusion (DMF) and Kurtosis Maximisation Fusion (KMF) techniques. They solve the cost functions based on two statistical parameters, i.e., the dispersion and the kurtosis, to estimate the weights. The conventional spatial domain fusion techniques based on spatial frequency, variance, energy of image gradient, information entropy, etc., are found in the works [8]-[11]. As far as the transform domain fusion techniques are concerned, the source images are first transformed into a new domain, then fused and the result is finally converted back by an inverse transform. Mahbubur Rahman *et al.* [3] calculate the weighted mean of wavelet coefficients of the source image for image

fusion, and the weights depend on the ratio of the local standard deviations of the detail and approximate coefficients. Cvejic *et al.* [12] calculate the weights by the mean absolute values of the Independent Component Analysis (ICA) coefficients, and then the weighted mean of the ICA coefficients for image fusion. Yang *et al.* [13] present an image fusion algorithm based on SR, and the sparse coefficients with maximum value of L_1-norm are chosen. From the above description, the image patches and the transform coefficients are combined respectively according to their activity indicator.

In the spatial domain techniques, the activity indicator of image patches is determined by some physical characteristics. So the spatial domain techniques are very intuitive and have the explicit physical meanings. According to the activity indicator, the image patches are combined with some rule. The fused image with the "choose-max" rule tends to be oversharp and less smooth, and the "weight average" rule is prone to make the fused image blurry [14]. It is a serious drawback to the spatial domain fusion techniques. The multiresolution image fusion methods overcome this problem well [15]. In the Discrete Wavelet Transformation (DWT) based fusion method, the low frequency coefficients considered as the activity of background are combined with the "weight average" rule, and the high frequency coefficients considered as the activity of foreground are chosen with the "choose-max" rule [16]. Since the measures of physical characteristics are subjected to noise disturbances, the performance of the spatial domain techniques will degrade drastically if the images to be fused contain noise. Some transformations such as DWT, ICA and SR have been significantly successful in the development of image denoising algorithms, so the transform domain fusion techniques are less influenced by noise. The activity indicator of the transformation coefficients are usually determined by some characteristic of the coefficients. The mathematic methods to express the characteristics of the coefficients are very limited and lack the explicit physical meanings. The spatial domain and the transform domain fusion techniques are remarkably complementary to one another in nature. A detailed state is given in Section II. Intuitively, the appropriate combined use of the two types of techniques can achieve better effect.

In this paper, we propose a combined sparse-spatial representation image fusion method. By combining the fusion techniques of the spatial domain and the transform domain, we carry forward the advantages and overcome the shortcomings of the two types of techniques. Our method first seeks an SR for each patch of all source images. Secondly, according to the input conditions, we adopt the appropriate spatial domain techniques to combine the dictionaries of the source images. Finally, the fused image can be reconstructed by the composite dictionary and the sparse coefficients. Since SR has strong ability to denoise, the proposed method can simultaneously carry out denoising and fusion of the images. The image patches can be represented as the linear combinations of some atoms in dictionary. The atoms are the essence elements of the image patches, so our method can combine the essence elements of the image patches. Furthermore, usually, since the number of atoms of dictionary is less than the dimension of coefficient matrix, our method has a potential to reduce the computational complexity. The rest of the paper is organized as follows. Section II gives a detailed state of image fusion in spatial domain and transform domain. Section III presents the description of the proposed image fusion method, whereas Section IV contains experimental results obtained by using the proposed method and a comparison with the state-of-the-art algorithms. The paper is concluded in section V.

2. Image fusion in spatial domain and transform domain

The image fusion process consists of three main steps: extracting image features, fusing these features with a certain rule, and constructing a fused image. The spatial domain techniques use the source image itself (or partial image) as image features, and combine the features with some rule. In the spatial domain techniques, some physical characteristics, such as the fuzziness [6], spatial frequency, variance, energy of image gradient, information entropy, etc., are applied to determine the activity indicator of image patches. So the spatial domain techniques often have the characteristics of less calculation, intuition and explicit physical meanings. According to the activity indicator, the image

patches are combined with some rule. Every image patch includes the foreground features (high activity level) and background features (low activity level). With the "choose-max" rule, the fused image will tend to be oversharp and less smooth. With the "weight average" rule, the foreground features in the fused image will be more blurred than in the source images. The above conclusions have been proven in detail in our previous work [14]. Moreover, in practice, the source images often contain the noise, and the measures of physical characteristics are subjected to noise disturbances, such that the fusion performance will degrade severely.

In the transform domain fusion methods, the source images are first transformed into a new domain and then fused. Finally, the result is converted back by an inverse transform. The activity indicator is often determined by some characteristics of the coefficients. The mathematic methods to express the characteristics of the coefficients are limited, lack explicit physical meanings, and mainly include L_2-norm, L_1-norm and the absolute value of the coefficients. The forward transform and backward transform increase the calculated amount, so the transform domain methods often have higher computational complexity than the spatial domain methods. However, the transform domain methods can overcome some drawbacks of the spatial domain methods. The DWT based image fusion method considers the low frequency coefficients of image patches as the background feature and the high frequency coefficients as the foreground feature, and combines them with the "weight average" rule and the "choose-max" rule respectively. Some transformations, such as DWT, ICA and SR, have strong ability to denoise, so there are fewer noises in their transformation coefficients. Thus, some transform domain fusion methods are less influenced by noise. Through the analysis above, we can get the conclusion that the spatial domain and the transform domain fusion methods have their special characteristics respectively and can compensate for each other.

3. Image fusion with a combined sparse-spatial representation method

In previous works [12] [13] and [16], the transform domain image fusion methods transfer the source images into a new domain, and combine the coefficients with the fusion rule. In this paper, a novel strategy is proposed. Instead of the coefficients, we adopt the appropriate spatial domain techniques to combine the dictionaries of the source images. The fused image can be constructed by the sparse coefficients and the combined dictionary. Sparse representation is a method that can describe most or all information of an image with a linear combination of a small number of atoms from dictionary. The atoms are considered as the essence elements of source images. Our method separates the elements into the common components and innovative components, and then combines them respectively. Furthermore, SR has stronger ability to remove noise. So our method is expected to overcome the drawbacks in the spatial domain fusion methods. The dictionaries are combined with the spatial domain techniques, such that our method has advantages of specific sense of physics. The number of atoms of dictionary is less than the dimension of coefficient matrix, so our method could reduce the computational complexity. Thus, our method has a potential to overcome the weakness of the transform domain fusion methods. Vinje and Gallant in [17] indicate that the primary visual cortex (area V1) uses a sparse code to efficiently represent natural scenes. Fusing image based on SR is appropriate in accordance with the human visual characteristic. In conclusion, according to the input conditions, the appropriate combined use of SR and the spatial domain techniques can achieve better fusion effect.

3.1 The dictionary joint training with K-SVD [18]

Since all the sparse coefficients of source images are same, the image features are present in the corresponding dictionaries. Let the pixels of the ideal images x_i $(i=1,2)$ to be fused be corrupted by an additive zero-mean white and homogeneous Gaussian noise n_i with known variances σ_i^2. The measured image s_i is thus

$$s_i = x_i + n_i \tag{1}$$

Each image is divided into $\sqrt{B}\times\sqrt{B}$ patches $s_i(l)$ $(l\in[1,L]$, $L=(M-\sqrt{B}+1)(N-\sqrt{B}+1))$ with sliding window technique. Each block is ordered lexicographically as vector $v_i(l)$. Assume that the vectors responding to all the patches in image s_i are constituted into one matrix V_i. The individual dictionary training problems are

$$\begin{cases}\min\limits_{D_1,\theta}\left\{\left\|V_1-D_1\theta\right\|_F^2\right\} & subject\ to\ \ \forall t,\quad \left\|\theta(l)\right\|_0\le T_0\\ \min\limits_{D_2,\theta}\left\{\left\|V_2-D_2\theta\right\|_F^2\right\} & subject\ to\ \ \forall t,\quad \left\|\theta(l)\right\|_0\le T_0\end{cases} \tag{2}$$

where $\theta(l)$ is the *l*-th column vector of θ and T_0 stands for the count of the nonzero entries in $\theta(l)$. In order to force the source images to share the same sparse coefficients, we train the dictionaries jointly. Let $\underline{V}=\begin{bmatrix}V_1\\V_2\end{bmatrix}$ and $\underline{D}=\begin{bmatrix}D_1\\D_2\end{bmatrix}$, then (2) can be rewritten as

$$\min_{\underline{D},\theta}\left\{\left\|\underline{V}-\underline{D}\theta\right\|_F^2\right\}\quad subject\ to\ \ \forall t,\quad \left\|\theta(l)\right\|_0\le T_0 \tag{3}$$

In this paper, we use the orthonormal matching pursuit (OMP) [19] to get an approximation solution of (3) because of its simplicity and fast execution.

3.2 Combining the dictionaries and constructing the fused image

In the next step, according to the input conditions, we adopt the spatial domain techniques to combine the atoms of dictionaries of the source images. In this paper, we use the feature indicator to evaluate the contribution of the atoms of dictionary instead of the activity indicator. Assume $D_1, D_2\in R^{B\times G}$, and let $I_i(g)$, $g=1,2,\cdots,G$ represent the innovation indicator of each atom. According to our previous work [14], the source image can be separated into the common components and the innovative components. And each image can be considered as the linear combination of some atoms of dictionary. In this paper, we regard the atoms as the common components if the difference between the innovation indicators of atoms corresponding to different images is small, otherwise as the innovative components. For the common components, we can use the "mean" rule. While for the innovative components, we combine the atoms with the "choose-max" rule, in order to try to preserve the features with the bigger feature indicator. Thus, the atoms of dictionary of fused image can be obtained by

$$D_F(g)=\begin{cases}D_1(g), & \text{if}\ \ I_1(g)>I_2(g)\ \text{and}\ \left|I_1(g)-I_2(g)\right|\ge\lambda\cdot\left(\left\|I_1(g)+I_2(g)\right\|\right)\\ D_2(g), & \text{if}\ \ I_1(g)\le I_2(g)\ \text{and}\ \left|I_1(g)-I_2(g)\right|\ge\lambda\cdot\left(\left\|I_1(g)+I_2(g)\right\|\right)\\ (D_1(g)+D_2(g))/2, & \text{otherwise}\end{cases} \tag{4}$$

Table I Various physical characteristics for different types of images

The types of images to be fused	The physical characteristics adopted
The medical images	Entropy [11], energy of image gradient [10] [20]
The multi-focus images	Spatial frequency [8], fuzziness [6], variance [9]
The infrared-visual images	Intensity [21], energy of image gradient [10] [20]

The image fusion methods in the existing literatures use various physical characteristics to fuse the images, as shown in Table 1. In this paper, according to the input conditions, these physical characteristics are adopted to determine the innovation indicator $I_i(g)$.

We can acquire the fused image dictionary D_F by calculating equation (4). Then the fused image matrix can be reconstructed by

$$V_F = D_F \theta \tag{5}$$

Finally, we can transform the matrix V_F to the image patches $x_F(l), l = 1, 2, \cdots, L$ and synthesize the fused image x_F by averaging the image patches in the same order the image patches were selected during the analysis step.

3.3 The computational complexity

The next, we compare roughly the computational complexity of our combined sparse-spatial representation method with the spatial domain methods and the transform domain methods. The computational complexity of the spatial domain methods comes from two parts: calculating the feature indicator and combining the features. In addition to two above sources, another contribution to the computational complexity of the transform domain methods is transforming the images forwardly and backwardly. For each pair of elements, we assume that the computational complexities of the feature indicator, the feature combination and image transformation can be represented by T_I, T_C and T_{Trans}. So the computational complexity of the spatial domain fusion methods is about

$$T_S = (T_I + T_C) \cdot L \tag{6}$$

and the computational complexity of the transform domain fusion methods is about

$$T_T = (T_I + T_C + T_{trans}) \cdot L \tag{7}$$

With our method, the images are fused by combining the dictionary instead of the coefficients, so the computational complexity is about

$$T_O = (T_I + T_C) \cdot G + T_{trans} \cdot L \tag{8}$$

In general, $G = L$ (for example, with the sliding windows technology, the image of size 256×256 will be divided into 62001 patches of size 8×8, and these patches can be represented in a dictionary of size 64×500. Thus $G = 500$ and $L = 62001$). So our method has a potential to offer a reduction in the computational complexity compared with the transform domain methods. If the algorithm of calculating the feature indicator is very sophisticated, the computational complexity of our method could even be lower than that of the spatial domain methods.

4. Experiments and comparisons

In this paper, the proposed fusion algorithm is compared with the spatial domain fusion methods and the transform domain fusion methods. The spatial domain methods based on entropy (EN) [11], spatial frequency (SF) [8], energy of image gradient (EG) [10] [20], intensity (IN) [21], and variance (VA) [9] have been proven to fuse the images well. The transform domain fusion methods, including sparse representation (SR)-based [13], the ICA [12] and discrete wavelet transform (DWT) [22]

methods are widely applied. In the proposed method, the overcomplete dictionary of size 64×500 is trained by K-SVD, the maximum number of iterations is set to 100, and $\lambda=0.5$. For a fair comparison, in all fusion methods, the source images are divided into small patches of size 8×8 using sliding window technique. In the SR based fusion algorithm, the fixed dictionary—an overcomplete DCT dictionary is applied and the sparse coefficients are estimated by OMP. The ICA algorithm are trained using 10 000 training patches selected randomly from a set of images with similar content, and 40 out of the most significant bases obtained by training are selected using the PCA algorithm. The DWT algorithm uses a five-level decomposition.

In order to evaluate the performance of these fusion algorithms, the objective fusion metric based on mutual information (Q_{MI}) [23], Petrovic's metric based on gradient of image (Q_G) [24], and Cvejie's metric (Q_C) [25] are applied. These metrics are calculated using the fused images and the corresponding noise-free images. The lager the values are, the better the fusion result will be.

The medical images are widely used in clinic diagnosis and treatment. MR and CT are important medical images. Due to the differences of the imaging principle between them, the dissection structure of showing they give prominence to differ. Normal and pathological soft tissue are better visualized by MR while the structure of bone, for example the temporal bone, including the middle ear and cochlea, is better visualized by CT. Because of the supplementary effects of MR and CT, the combination of the two types of images can often lead to additional clinical information not apparent in the separate images.

Fig. 1 shows the medical images corrupted with Gaussian noise, and their fused images using the fusion methods based on ICA, SR, DWT, EN, EG and our method. In our method, the feature indicator is determined by the energy of image gradient. It can be seen that, the fused images in Fig. 5(c), (e) and (h) are better perceptive than the fused results of other methods in Fig. 5(d), (f) and (g). Our method, SR and EG have successfully chosen the soft tissues features in the MR image and the hard tissues features in the CT image. The fused image with EG contains more noise than that with our method and SR. The structure of soft tissues of fused images by EN is clear, but the structure of bones is blurred. For DWT and ICA, the contrast is reduced to some extent and the edges are not easily distinguished.

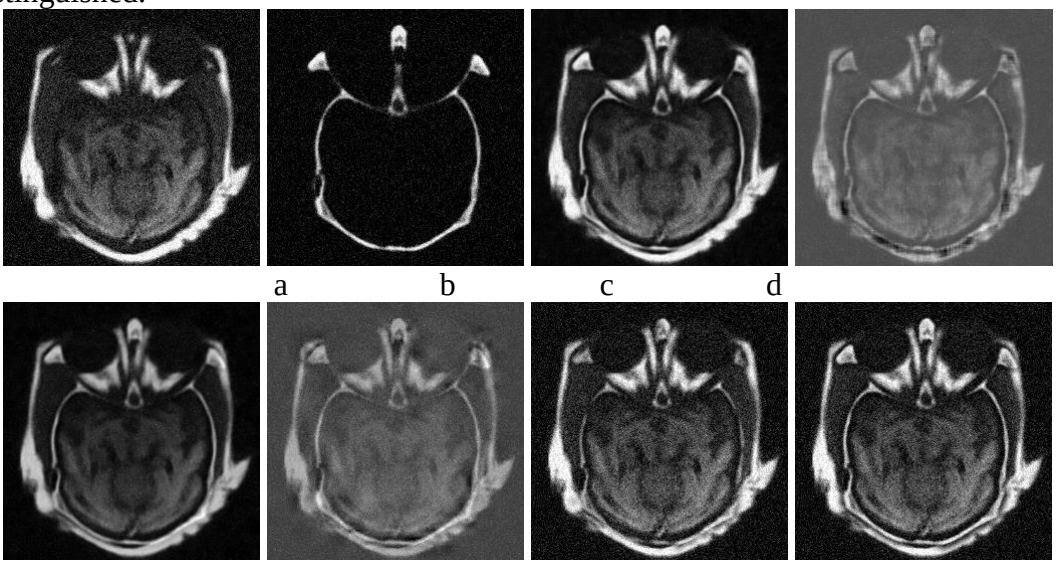

Fig. 1 Visual comparison of the performance of the fusion algorithms using the medical images corrupted with Gaussian noise, $\sigma=[20, 20]$. (a) Input magnetic resonance (MR) image. (b) Input computed tomography (CT) image. (c) The fused image, the proposed algorithm. (d) The fused image, ICA fusion algorithm. (e) The fused image, SR fusion algorithm. (f) The fused image, DWT fusion algorithm. (g) The fused image, EN fusion algorithm. (h) The fused image, EG fusion algorithm.

The corresponding standard fusion metrics, including Q_{MI}, Q_C and Q_G, are listed in Table II. The highest quality measures obtained over all methods are indicated by the values in bold. From Table II, we can see that our method provides higher values in Q_C and Q_G, and is a little inferior to SR in Q_{MI}.

Table II Performance of image fusion methods by the standard fusion metrics for medical images

Image	Medical image		
Metric / Method	Q_{MI}	Q_C	Q_G
Our method	0.4926	0.4661	0.9302
ICA	0.3936	0.2793	0.7494
SR	0.5076	0.4237	0.8723
DWT	0.3474	0.2823	0.8028
EN	0.3810	0.3650	0.9131
EG	0.3745	0.3689	0.9087

Since the optical lenses, particularly those with long focal lengths, suffer from the problem of limited depth of field, it is impossible to get an image in which all containing objects appear sharp. The objects in front of or behind the focus plane would be blurred. Multi-focus image fusion can get one image with all the objects focused.

Fig. 2 shows the multi-focus images corrupted with Gaussian noise, and their fused images using ICA, SR, DWT, SF, VA and the proposed method. In our method, the feature indicator is determined by the spatial frequency. Fig. 7(a) is near focused, where the small clock is in focus and clear in vision, whereas the big clock is out of focus and blurred. Fig. 7(b) is far focused, and the situations for the small clock and the big clock are contrary. We can see that all the objects of the fused image provided by our method and SF are sufficiently well focused, and both the big and small clocks look clearer. Compared with SF, the noise of the fused image with our method has been removed significantly.

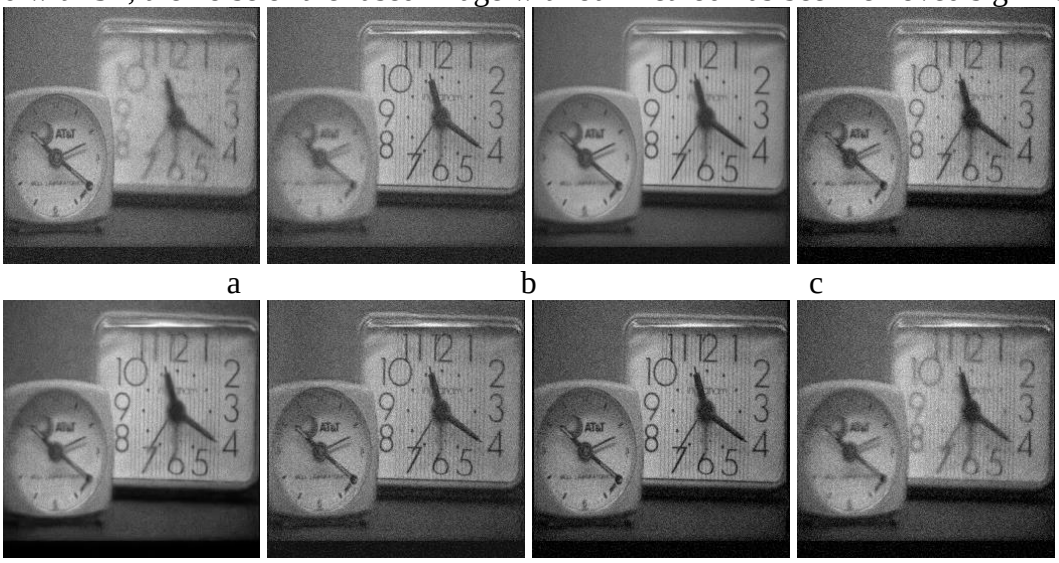

a b c d

e f g h

Fig. 2 Visual comparison of the performance of the fusion algorithms using the multi-focus images "Clock" corrupted with Gaussian noise, $\sigma = [10, 10]$. (a) and (b) Multi-focus "Clock" images. (c) The fused image, the proposed algorithm. (d) The fused image, ICA fusion algorithm. (e) The fused image, SR fusion algorithm. (f) The fused image, DWT fusion algorithm. (g) The fused image, SF fusion algorithm. (h) The fused image, VA fusion algorithm.

In Table III, we show the fusion metrics for two pairs of multi-focus images. In most cases, our method obtains the highest value, only lost to SR in Q_{MI} for the multi-focus images "Clock". It is in line with the visual effects.

Table III Performance of image fusion methods by the standard fusion metrics for multi-focus images

Image	Clock			Book		
Metric / Method	Q_{MI}	Q_C	Q_G	Q_{MI}	Q_C	Q_G
Our method	0.7863	0.6216	0.9673	1.0098	0.7978	0.9703
ICA	0.6529	0.5191	0.9690	0.6722	0.6418	0.9258
SR	0.7984	0.6193	0.9700	0.9089	0.7135	0.9700
DWT	0.6051	0.5026	0.9657	0.9241	0.7247	0.9702
SF	0.6528	0.5211	0.9639	0.6827	0.5799	0.9659
VA	0.6502	0.5024	0.9584	0.6698	0.5796	0.9646

5. Conclusions

In this paper, we propose a combined sparse-spatial representation method, which seeks a SR for each patch of all source images, and then uses the sparse coefficients and the composite dictionary to generate the fused image. With SR, the essence elements of the images can be extracted. These elements are considered as image features, and combined with different rules according to the feature indicators. Since the dimension of dictionary is usually less than that of the coefficient matrix, our method has a potential to cut down the amount of calculation. Experiment results show that the proposed method has better fusion performance than the state-of-the-art methods.

Acknowledgment

This work was supported by the Nature Science Foundation of the Jiangsu Higher Education Institutions of China (Grant No. 13KJB51-0010), the Nature Science Foundation of Jiangsu province, China (Grant No. BK20130230) and the Nature Science Foundation of China (Grant No. 61401181).

References

[1] K. Mrityunjay, Optimal image fusion using the rayleigh quotient, *IEEE Sensors Applications Symposium*, New Orleans, LA, USA, 2009, pp. 1-6.

[2] N. Cvejic, T. Seppänen and S. J. Godsill, A Nonreference Image Fusion Metric Based on the Regional Importance Measure, *in IEEE Journal of selected topics in signal Processing*, vol. 3, no. 2, pp. 212-220, April 2009.

[3] S. M. Mahbubur Rahman, M. Omair Ahmad, and M. N. S. Swamy, Contrast-based fusion of noisy images using discrete wavelet transform, *IET Image Process.*, vol. 4, iss. 5, pp. 374-384, 2010.

[4] S. Nikolov, D. Bull, and N. Canagarajah, Wavelets for image fusion, in *Wavelets in Signal and Image Analysis*. Norwell, MA: Kluwer, 2001.

[5] V. Aslantas, R. Kurban, Fusion of multi-focus images using differential evolution algorithm, Expert Systems with Applications (2010), doi:10.1016/j.eswa.2010.06.011.

[6] R. Maruthi, Spatial Domain Method for Fusing Multi-Focus Images using Measure of Fuzziness, International Journal of Computer Applications, vol. 20, no. 7, pp. 48-51, April, 2011.

[7] Oudre L., Stathaki T., Mitianoudis N., Image Fusion Using Optimization of Statistical Measurements, Book chapter, Image fusion: Algorithms and Applications, Academic Press, pages 520, 2008.

[8] S. Li, B. Yang, Multifocus image fusion using region segmentationand spatial frequency, Image and Vision Computing, vol. 26, iss. 7, July, 2008, pp. 971-979.

[9] Y. Zhang, L. Ge, An efficient fusion scheme for multi-focus images by using blurring measure, Digital Signal Processing, vol. 19, iss. 2, March, 2009, pp. 186-193.
[10] VS. Petrovic, CS. Xydeas, Gradient-Based Multiresolution Image Fusion, IEEE TRANSACTIONS ON IMAGE PROCESSING, vol. 13, no. 2, Feb. 2004, pp. 228-237.
[11] N. Cvejic, C. N. Canagarajah, D.R. Bull, Image fusion metric based on mutual information and Tsallis entropy, ELECTRONICS LETTERS, vol. 42, no. 11, May, 2006, pp. 1-2.
[12] N. Cvejic, D. Bull, N. Canagarajah, Region-based multimodal image fusion using ICA bases, IEEE Sens. J. , vol. 7, no. 5, pp. 743–751, 2007.
[13] B. Yang, and S. Li, Multifocus Image Fusion and Restoration with Sparse Representation, *IEEE Trans. Instrumentation and Measurement*, vol. 59, no. 4, pp. 884-891, April 2010.
[14] N. Yu, T. Qiu, F. Bi, A. Wang, Image features Extraction and Fusion Based on Joint Sparse Representation, IEEE Journal of selected topics in signal processing, vol. 5, no. 5, 2011, pp. 1074-1082.
[15] G. Piella, A general framework for multiresolution image fusion: From pixels to regions, Research Report PNA-R0211, Centrum voor Wiskun de en Informatica (CWI), Amsterdam, Netherlands, 2002.
[16] S. Zhu, IMAGE FUSION USING WAVELET TRANSFORM, Symposium on Geospatial Theory, Processing and applications, Ottawa 2002, pp. 1-5.
[17] W. E. Vinje, J. L. Gallant. Sparse coding and decorrelation in primary visual cortex during natural vision, Science, 2000, 287, pp.1273–1276.
[18] M. Aharon, M. Elad, and A. Bruckstein, *K*-SVD: An algorithm for designing overcomplete dictionaries for sparse representation, *IEEE Trans. Signal Process.*, vol. 54, no. 11, pp. 4311–4322, November 2006.
[19] Y. C. Pati, R. Rezaiifar, and P. S. Krishnaprasad, Orthogonal matching pursuit: Recursive function approximation with applications to wavelet decomposition, in *Conf. Rec. 27th Asilomar Conf. Signals, Syst. Comput.*, 1993, vol. 1.
[20] X. Zhang, Research on multi-mode medical image fusion algorithm based on wavelet transform and the edge characteristics of images, Image and Signal Processing, 2009. CISP '09. 2nd International Congress on, 17-19 Oct. 2009, Tianjin, China.
[21] D. Drajic, N. Cvejic, Adaptive fusion of multimodal surveillance image sequences in visual sensor networks, IEEE Transactions on Consumer Electronics, vol. 53, iss. 4, 2007, pp. 1456-1462.
[22] G. Pajares, J.M. de la Cruz, A wavelet-based image fusion tutorial, Pattern Recognition 37 (9) (2004) 1855–1872.
[23] G. Qu, D. Zhang, P. Yan, InformationMeasurefor Performance of Image Fusion, Electronics Letters, vol. 38, no. 7,pp. 313-315, 2002.
[24] V. Petrovic, Subjective Tests for Image Fusion Evaluation and Objective Metric Validation, Information Fusion, vol. 8, no. 2, pp. 208-216, 2007
[25] N. Cvejic, A. Loza, D. Bul, and N. Canagarajah, A Similarity Metric for Assessment of Image Fusion Algorithms, Int'l J. Signal Processing, vol. 2, no. 3, pp. 178-182, 2005
[26] The Image Fusion Server. [Online]. Available: http://www.imagefusion.org/